LAWRENCE
LIVERMORE
NATIONAL
LABORATORY

UCRL-JRNL-217068

Laser-driven shock experiments in pre-compressed water: Implications for magnetic field generation in Icy Giant planets

K. Lee, L. R. Benedetti, R. Jeanloz, P. M. Celliers, J. H. Eggert, D. G. Hicks, S. J. Moon, A. Mackinnon, E. Henry, M. Koenig, A. Benuzzi-Mounaix, G. W. Collins

November 14, 2005

Journal of Chemical Physics

Updated October 14, 2003

Laser-driven shock experiments in pre-compressed water: Implications for magnetic field generation in Icy Giant planets

Kanani K. M. Lee[1, 2*], L. Robin Benedetti[3, 4], Raymond Jeanloz[1], Peter M. Celliers[4], Jon H. Eggert[4], Damien G. Hicks[4], Stephen J. Moon[4], Andrew Mackinnon[4], Emeric Henry[5], Michel Koenig[5], Alessandra Benuzzi-Mounaix[5], Gilbert W. Collins[4]

[1]Department of Earth & Planetary Science, University of California, Berkeley, 307 McCone Hall, Berkeley, CA 94720-4767 USA

[2]Division of Geological & Planetary Sciences, California Institute of Technology, 1200 E. California Blvd., Pasadena, CA 91125 USA

[3]Physics Department, University of California, Berkeley, 366 LeConte Hall, Berkeley, CA 94720-7300 USA

[4]Lawrence Livermore National Laboratory, 7000 East Avenue, Livermore, CA 94550, USA

[5]Laboratoire LULI, Ecole Polytechnique, 91128 Palaiseau, France

[*]To whom correspondence should be addressed. Email: kanani@gps.caltech.edu

Abstract

Laser-driven shock compression of pre-compressed water (up to 1 GPa pre-compression) produces high-pressure, -temperature conditions in the water inducing two optical phenomena: opacity and reflectivity in the initially transparent water. The onset of reflectivity at infrared wavelengths can be interpreted as a semi-conductor to electronic conductor transition in water and is found at pressures above ~130 GPa for single-shocked samples pre-compressed to 1 GPa. This electronic conduction provides an additional contribution to the conductivity required for magnetic field generation in Icy Giant planets like Uranus and Neptune.

Introduction

Although the giant gas planets are mostly comprised of hydrogen and helium, the Icy Giants Neptune and Uranus are additionally believed to contain as much as ~50% water (by mass) and significant amounts of methane and ammonia.[1] Most of the water is in a dense, fluid state, forming an "icy" interior layer with pressures ranging between 20 and 600 GPa and temperatures between 2500 and 7000 K (Figure 1).[1] "Ice" refers to the presence of molecular species, such as water, methane or ammonia, and it is hypothesized that it is in this icy layer that the planet's magnetic field is produced.[1]

Understanding the origin and mechanisms of planetary magnetic fields is important as they are prevalent in our solar system, and can be expected to be important in extra-solar planets as well.[2] Magnetic fields are produced by three mechanisms: permanent magnetism, which is produced at the microscopic level and is inherent to the material (e.g., ferromagnetism); induction from external sources; or by production through electrical currents generated by a dynamo. Although some of the magnetism in our Solar System can be attributed to permanent magnetism from iron-rich minerals (e.g., Moon and Mars) or by induction by varying external magnetic fields (Galilean satellites), most must be formed by a dynamo sustained by convection of an electrically conducting fluid deep inside the planet. Together with moment of inertia measurements, magnetic field observations can be used to constrain chemical makeup and interior processes.

The magnetic fields of Neptune and Uranus were first measured during the Voyager 2 mission.[3] The surface field was shown to be about the same for both planets, ~2 x 10^{-5} T, comparable in strength to the Earth's magnetic field value of ~5 x 10^{-5} T. Although it is expected that the Icy Giants have a core of ice, rock and metal about the

size of the Earth, the mostly quadrupolar nature of the observed magnetic field suggests that an Earth-like iron-dominated geodynamo near the center of the planet is unlikely to be the source of the magnetism as the quadrupole term falls as r^{-4} in field strength, where r is radius. The large radius of an Icy Giant planet dictates that for such a strong quadrupole field to be measured, the source must be at shallower depths. It is thought that an ionic or perhaps metallic form of water, existing at high pressures (20-600 GPa) and temperatures (2500-7000 K) in the shallower depths (~6000-17,000 km deep) of the planet, sustains the necessary electric currents for the planetary dynamo (Figure 1).[1] Current estimates suggest that a minimum conductivity of ~10 $(\Omega\text{-cm})^{-1}$ is required to generate the observed magnetic field.[4] Conductivity values of this magnitude have been measured for both shock-compressed water[5-7] and for a mixture of ices called "Synthetic Uranus.[8]" A larger value of conductivity relaxes the velocity and length scales for a self-sustaining dynamo.[2] A recent dynamo model finds that in order to match the magnetic field morphology for a planet like Neptune or Uranus, the dynamo is formed by a thin, conducting, fluid shell above a stably-stratified, conducting, fluid interior and small solid core.[9]

The high-pressure and high-temperature environment of planetary interiors has been simulated in the laboratory with diamond-anvil cells (DAC) and shock-wave experiments. Successful DAC experiments on water have been carried out to 210 GPa at temperatures near 300 K[10,11] and at lower pressures but higher temperatures,[12-18] leaving much of the pressure range relevant to the icy layer uninvestigated (Figure 1). Shock waves produce high pressures and temperatures in the sample for a short period of time (ns – μs). Unfortunately, the temperatures reached through single-shock wave

compression tend to be much higher than that of the interior layer of ice. Early Soviet strong-shock wave experiments (produced by nuclear explosions) reached up to 3.2 TPa in water.[19,20] More recently, laser-driven shock experiments on water have reached pressures up to nearly 800 GPa with estimated temperatures greater than 30,000 K.[21] Reverberating shock wave experiments on water have reached 180 GPa[5,7] and ~5400 K (temperature reevaluated in separate study[21]). Previous single-shock gas gun experiments were limited to pressures below 100 GPa.[6,22-24]

Static compression typically yields an equation of state (EOS) along an isotherm, while dynamic (shock wave) methods probe the EOS along a Hugoniot yielding density and internal energy information along a well-defined pressure-temperature (P-T) path. Shock wave methods tend to produce strong heating and high temperatures, usually too high to be useful for studying planetary isentropes. On the other hand, static methods are difficult to implement at temperatures greater than ~3000 K. By combining dynamic and static methods, laser-driven shock wave experiments on pre-compressed samples access conditions unreachable by either static DAC or dynamic single-shock wave techniques alone, and allow the investigation of a broad range of P-ρ-T space.[25,26] Knowing the initial pressure and density of the pre-compressed sample, it is possible to infer the P-ρ-E conditions achieved in the sample under shock compression via the Rankine-Hugoniot relations: [27]

$$\rho_0 U_S = \rho_1 \left(U_S - u_p \right) \tag{1}$$

$$P_1 - P_0 = \rho_0 U_S u_p \tag{2}$$

$$E_1 - E_0 = \frac{1}{2}\left(P_0 + P_1\right)\left(\frac{1}{\rho_0} - \frac{1}{\rho_1}\right) \tag{3}$$

where ρ is density, U_S is shock velocity, u_p is particle velocity, P is pressure, E is internal energy and subscripts 0 and 1 are the initial and final states. Equations 1-3 are the conservation of mass, momentum and energy relations.

Here we present EOS and optical measurements using laser-driven shock waves on pre-compressed samples of water. The EOS measurements lie between the principal isentrope and principal Hugoniot of water, due to the increased initial density of the pre-compressed sample, thereby better producing conditions closer to those of the icy layers of Neptune and Uranus. We also observe optical changes in the shock-compressed water from transparent to opaque to reflecting, providing evidence for a change in the electrical conduction mechanism in H_2O under conditions relevant for the production of magnetic fields in the Icy Giant planets.[21,28]

Methods

The sample consists of a layer of doubly-distilled ultra-pure water compressed between two diamond windows, with a stepped aluminum foil embedded in the water layer and placed against the diamond window from which the shock wave enters (Figure 2). The aluminum foil is used for calibration of the shock-wave velocity and is stepped, such that the shock wave traverses two distinct thicknesses before entering the water.[21,25,26] Modified DACs fit with 200-500 μm thick, 1.0 mm in diameter diamond windows, were used to compress water to a finite initial density and pressure (see Table 1) and were shocked by a high-power laser pulse.[29] A detailed description of the design of the pre-compressed targets has been given elsewhere.[25] These experiments were performed at the Vulcan Laser Facility at the Rutherford Appleton Laboratory.[29] Shots

identified with a "00" prefix were driven with a 4-ns square laser pulse composed of a series of stacked 1-ns pulses, whereas a "01" prefix identifies experiments driven with a 1-ns square pulse. The longer duration pulses yield a more steady shock throughout the sample; the short pulses provide stronger shocks due to the increased power density of the laser pulse.

For each shot, there were three probes monitoring the sample: two VISAR (Velocity Interferometer System for Any Reflector) interferometers (Figures 3, 4) and an optical pyrometer.[26,30-32] For all "00" shots, both interferometers were operated at 532 nm, whereas all "01" shots were recorded by an interferometer operating at 532 nm and a second operating at 1064 nm. A streaked optical pyrometer was also used to measure the blackbody radiation emitted from the shocked sample. The absolute calibration on the pyrometric measurement was not accurate enough to determine temperatures to better than ~35% uncertainty at the highest pressures. For this reason we calculate the temperatures of the shocked pre-compressed water using the model of Ree,[33] available in the SESAME database,[34] T_{SESAME} (Table 1). This equation of state model matches the measured principal Hugoniot of water to over 800 GPa[21]; we use it to estimate the shock temperatures for water off the principal Hugoniot.

Analysis

The analysis of the VISAR records reveals changes in the optical properties in water from its initially transparent state: with increasing shock pressures and temperatures, water became optically opaque (T_{SESAME} > ~3000 K) then reflecting (T_{SESAME} > ~6000 K). Because VISAR requires a reflecting surface, the changing optical

properties of the sample must be considered and are described below for each optical character observed. Reflectivity is estimated by determining the intensity of light measured after the shock breaks out from the Al step (reflectivity of ~80% in a spectral range of 550-580 nm).[35] In samples that remain transparent (T_{SESAME} < ~3000 K), the intensity of the light after breakout is nearly the same (within 5% of unshocked Al intensity); that is, the water continues to stay transparent to the light being reflected off the moving Al step (Figure 3). For opaque samples (~3000 K < T_{SESAME} < ~6000 K), the intensity of light after breakout from the Al step drops to less than 5% of the unshocked Al intensity, within an absorption depth of less than 1 μm. Samples identified as reflecting were observed to reflect the probe from the shock front rather than from the moving Al-water interface and are identified as such with Al shock velocities that are greater than those that have been identified as opaque (Figure 4; Table 1). Uncertainties in the absolute value of the reflectivity are significant (up to 20-40%) owing to imperfections in the Al step surface and anti-reflection coatings, as well as the presence of ice VI crystal formation for the highest pre-compression pressures. However, the onset of reflectivity was clearly observed at a detection limit of ~3-5%. Initial conditions, measured and calculated velocities, and final conditions as determined by the Rankine-Hugoniot relations and impedance matching[27] are listed in Table 1.

Results

We measure the shock velocity of Al, U_S(Al), by measuring the transit time between the breakout times in the low and high steps of the Al stepped foil of known thickness, measured by white light interferometry before and after pre-compression. The thickness of the step height does not change appreciably due to the low pre-compression

pressures and relatively high bulk modulus of Al. We calculate the particle velocity of the Al, u_p(Al), from a fit to existing absolute Hugoniot data for Al: U_s=5.448 + 1.324 u_p, for $u_p \leq 6.763$; U_s=6.511 + 1.167 u_p, for $u_p > 6.763$ (velocities in km/s) <<reference Celliers et al., Journal of Applied Physics, accepted for publication>>. For transparent samples, it is also possible to infer the particle velocity in the water, $u_p(H_2O)$, from the VISAR data.[30,32,37,38] Uncertainties in the U_S(Al) determination are reduced due to the redundant interferometers, but can be as large as 5%. To determine the conditions reached in the shocked pre-compressed water, we use impedance matching techniques[27] and the SESAME tables.[33,34]

Water remains transparent along the principal Hugoniot beyond 30 GPa <<include the following reference: Ya. B. Zel'dovich et al., Sov. Phys. Dokl., **6**, 494 (1961)>>.[24] In one of our shots, we find that water remains transparent at pressures exceeding 100 GPa at temperatures less than 3000 K. In this shot, 001212-13 (Figure 3), we observe a leading shock as it is overtaken by a stronger following shock. The first discontinuity in the VISAR image is the first shock wave as it breaks through the Al step into the pre-compressed water: the water remains transparent and the observed reflection originates from the Al-water interface. The next discontinuity indicates the arrival of the second shock at the Al-water interface, and the final discontinuity indicates the second shock overtaking the first shock, producing conditions that make the water opaque. Calculations designed to match the observed interface velocities indicate that the two shocks compressed the sample to two distinctive P-T conditions where the water continues to be transparent: ~47 GPa and 2100 K and ~125 GPa and 2800 K.

Deleted: ,

At pressures above ~50 GPa along the principal Hugoniot previous studies have observed water to become opaque.[22] We also observe water to be opaque at estimated temperatures > 3000 K. The opacity of the water is confirmed by a low reflectivity (low intensity fringes remain as a result of ghost reflections from the external surface of the diamond window) and the lack of fringe shift after the Al shock breakout in both VISAR records.

An example of a reflecting VISAR record is shown in Figure 4. The first two fringe discontinuities are due to the Doppler shift of the moving Al-water interface. Since the reflected light originates from the shock front, the fringe shift yields the shock velocity in the water, U_S(water). As the water is pre-compressed, the pressure-dependent index of refraction of water was taken into account in determining the shock velocities (n = 1.37 – 1.45 at our initial compressions of 0.40-1.02 GPa).[39],[32] We also observe the reflectivity to decrease as the shock wave strength decays, with the sample becoming opaque in the infrared at ~130 GPa along the pre-compressed 1 GPa Hugoniot (Figures 4, 5). This is similar to reflectivity observations along the principal Hugoniot found earlier.[21] With these observations, the optical transition from opaque to reflecting is found to be pressure and temperature dependent yielding a transition slope of approximately -12 K/GPa, although the uncertainties are large and could be as much as ±9 K/GPa.

Discussion

In previous work[21] we modeled the reflectivity using a standard semiconductor formulism to estimate the free carrier density and a Drude model to calculate the

electronic conductivity σ_e. In this model, we empirically fit reflectivity data at 532 nm and 1064 nm along the principal Hugoniot and calculated the free carrier density and σ_e. A linear temperature and density dependence of the gap energy was included in the fit.[21] We find this model is consistent with our current observations of shocked pre-compressed water and is used in our current analyses.

In Figure 5, we plot the 1, 10, 100 and 1000 $(\Omega\text{-cm})^{-1}$ electronic conductivity contours as we calculate using this model. The observed reflectivity can thus be attributed to the production of thermally-activated electrons (i.e. semiconducting behavior). Our observations are consistent with reflectivity observed for laser-driven single-shock experiments on the principal Hugoniot at pressures above 100 GPa where temperatures are higher at any given pressures (Figure 5),[21] and suggest that the model can be expected to represent the electronic conductivity along the isentrope accurately. If the onset of reflectivity is an indication of an increased electronic contribution to the conductivity, and is both pressure and temperature dependent, our new measurements and model help to constrain the relative contributions of ionic and electronic conductivity along the Icy Giant isentrope. From the model, the 10 $(\Omega\text{-cm})^{-1}$ σ_e contour intersects the Neptune isentrope near 125 GPa, while the 100 $(\Omega\text{-cm})^{-1}$ σ_e contour, a conductivity value approaching that of a poor metal, intersects the isentrope near 250 GPa. This suggests that the conductivity in the outer layers in sufficient for dynamo production and operates through a combination of electronic and ionic conduction mechanisms.

Our results compare well with previous observations of the optical properties of water under high pressure and temperature conditions. Early shock-wave experiments on water along the principal Hugoniot have also observed transparency <<include the

following reference: Ya. B. Zel'dovich et al., Sov. Phys. Dokl., **6**, 494 (1961)>>,[24] opacity[22] and reflectivity.[21] Early optical studies of shock compressed water found the samples to be transparent as high as 30 GPa.<<Zel'dovich reference>> A Raman study of shocked water up to 26 GPa and 1700 K required a transparent sample.[24] Recent Raman spectroscopy experiments on DAC water samples observe transparent water up to 56 GPa and 1500 K and interpret their spectra as evidence of superionicity.[15] However, above 50 GPa on the principal Hugoniot (~ 3000 K) thermal emissivity measurements indicate that water bevomes opaque at these conditions[22] (see Figure 5). DAC water samples compressed between 6 and 43 GPa and heated to temperatures above ~2000 K were also observed to be opaque.[12]

Conclusions

We observe three distinct regimes of differing optical properties upon shock compression: transparent, opaque and reflecting (see Table 1, Figure 5). At low temperatures (T < ~3000 K), the shocked water remains transparent with VISAR measuring the Al-sample interface. With increasing shock pressure, the sample becomes opaque (optically thick) and can be interpreted as a semiconductor. With further increased pressures, and therefore increased temperatures, the shocked water becomes reflecting and is electronically conducting. This has been observed in previous experiments,[21] and is interpreted as the onset of electronic conduction in water caused by the high temperatures reached during shock loading. At pressures and temperatures greater than ~130 GPa and 6600 K, water becomes reflecting at 1064 nm although still opaque at 532 nm. At the most extreme pressure and temperature that we achieved, ~250 GPa and ~19,000 K (T_{SESAME}), we observe water reflecting at visible wavelengths.

Figure 5 shows our measurements compared with the phase diagram of water based on *ab-initio* molecular dynamic calculations.[28] Some of our measurements cluster near Neptune's expected isentrope, and suggest that, in addition to the ionic conduction mechanism, a temperature-activated semi-conducting contribution must be included in the total electrical conductivity at pressures > 120 GPa. Our results provide additional evidence that water can sustain a magnetic dynamo at fairly shallow levels in the planet and within the icy mantle, compatible with the strongly quadrupolar nature of the observed magnetic field.[3]

Acknowledgements. We thank Paul Loubeyre and Agnes Dewaele for extensive experimental and technical help. We thank Walt Unites and the operations staff of the Vulcan Laser Facility at Rutherford Appleton Laboratory for their support. This research was supported by the National Science Foundation and under the auspices of the U.S. Department of Energy by the University of California, Lawrence Livermore National Laboratory through the Institute of Laser Science and Application, under contract No. W-7405-Eng-48.

References

[1] W. B. Hubbard, *Planetary Interiors*. (Van Nostrand Reinhold Company, New York, 1984).
[2] D. J. Stevenson, Earth Planet. Sci. Letts 208, 1 (2003).
[3] E. C. Stone and E. D. Miner, Science 246 (4936), 1417 (1989).
[4] R. L. Kirk and D. J. Stevenson, Astrophys. J. 316, 836 (1987).
[5] V. V. Yakushev, V. I. Postnov, V. E. Fortov, and T. I. Yakysheva, Journal of Experimental and Theoretical Physics 90 (4), 617 (2000).
[6] A. C. Mitchell and W. J. Nellis, J. Chem. Phys. 76 (12), 6273 (1982).
[7] R. Chau, A. C. Mitchell, R. W. Minich, and W. J. Nellis, J. Chem. Phys. 114 (3), 1361 (2001).
[8] W. J. Nellis, N. C. Holmes, A. C. Mitchell, D. C. Hamilton, and M. Nicol, J. Chem. Phys. 107 (21), 9096 (1997).
[9] S. Stanley and J. Bloxham, Nature 428, 151 (2004).
[10] A. F. Goncharov and V. V. Struzkhin, Science 273 (5272), 218 (1996).
[11] R. J. Hemley, A. P. Jephcoat, H. K. Mao, C. S. Zha, L. W. Finger, and D. E. Cox, Nature 330, 737 (1987).
[12] L. R. Benedetti, PhD thesis, University of California, Berkeley, 2001.
[13] B. Schwager, L. Chudinovskikh, A. Gavriliuk, and R. Boehler, J. Phys.: Cond. Matt. 16, S1177 (2004).
[14] J.-F. Lin, B. Militzer, V. V. Struzkhin, and E. Gregoryanz, J. Chem. Phys. 121 (17), 8423 (2004).
[15] A. F. Goncharov, N. Goldman, L. E. Fried, J. C. Crowhurst, I.-F. Kuo, W., C. J. Mundy, and J. M. Zaug, Phys. Rev. Lett. 94, 125508 (2005).
[16] M. R. Frank, Y. Fei, and J. Hu, Geochimica et Cosmochimica Acta 68 (13), 2781 (2004).
[17] T. Kawamoto, S. Ochiai, and H. Kagi, J. Chem. Phys. 120 (13), 5867 (2004).
[18] Y. Fei, H. K. Mao, and R. J. Hemley, J. Chem. Phys. 99 (7), 5369 (1993).
[19] E. N. Avrorin, B. K. Vodolaga, L. P. Volkov, A. S. Vladimirov, V. A. Simonenko, and B. T. Chernovolyuk, JETP Letters 31 (12), 727 (1980).
[20] M. A. Podurets, G. V. Simakov, R. F. Trunin, L. V. Popov, and B. N. Moiseev, Sov. Phys. JETP 35 (2), 375 (1972).
[21] P. M. Celliers, G. W. Collins, D. G. Hicks, M. Koenig, E. Henry, A. Benuzzi-Mounaix, D. Batani, D. K. Bradley, L. B. Da Silva, R. J. Wallace, S. J. Moon, J. H. Eggert, K. K. M. Lee, L. R. Benedetti, R. Jeanloz, I. Masclet, N. Dague, B. Marchet, M. Rabec Le Gloahec, C. Reverdin, J. Pasley, O. Willi, D. Neely, and C. Danson, Phys. Plasmas 11 (8), L41 (2004).
[22] G. A. Lyzenga, T. J. Ahrens, W. J. Nellis, and A. C. Mitchell, J. Chem. Phys. 76 (12), 6282 (1982).
[23] L. P. Volkov, N. P. Voloshin, R. A. Mangasarov, V. A. simonenko, G. V. Sin'ko, and V. L. Sorokin, JETP Letters 31 (9), 513 (1980).
[24] N. C. Holmes, W. J. Nellis, and W. B. Graham, Phys. Rev. Lett. 55 (22), 2433 (1985).

[25] K. K. M. Lee, L. R. Benedetti, A. Mackinnon, D. G. Hicks, S. J. Moon, P. Loubeyre, F. Occelli, A. Dewaele, G. W. Collins, and R. Jeanloz, Shock Compression Condensed Matter (2002).
[26] P. Loubeyre, P. M. Celliers, D. G. Hicks, E. Henry, A. Dewaele, J. Pasley, J. Eggert, M. Koenig, F. Occelli, K. K. M. Lee, R. Jeanloz, D. Neely, A. Benuzzi-Mounaix, D. Bradley, M. Bastea, S. J. Moon, and G. W. Collins, High P High Temp 24 (1), 25 (2004).
[27] Y. B. Zeldovich and Y. P. Raizer, *Physics of shock waves and high temperature phenomena*. (Academic Press, New York, 1967).
[28] C. Cavazonni, G. L. Chiarotti, and S. Scandolo, Science 283 (5398), 44 (1999).
[29] I. N. Ross, M. S. White, J. E. Boon, D. Craddock, A. R. Damerell, R. J. Day, A. F. Gibson, P. Gottfeldt, D. J. Nicholas, and C. J. Reason, IEEE Journal of Quantum Electronics QE-17 (9), 1653 (1981).
[30] L. M. Barker and R. E. Hollenbach, J. Appl. Phys. 43 (11), 4669 (1972).
[31] P. M. Celliers, G. W. Collins, L. B. DaSilva, D. M. Gold, and R. Cauble, Appl. Phys. Lett. 73, 1320 (1998).
[32] P. M. Celliers, D. K. Bradley, G. W. Collins, D. G. Hicks, T. R. Boehly, and W. J. Armstrong, Rev. Sci. Instr. 75 (11), 4916 (2004).
[33] F. H. Ree, Lawrence Livermore National Laboratory Report Report No. UCRL-52190, 1976.
[34] S. P. Lyon and J. D. Johnson, Los Alamos National Laboratory Report Report No. LA-UR-92-3407, 1992.
[35] A. V. Bessarab, N. V. Zhidkov, S. B. Kormer, D. V. Pavlov, and A. I. Funtikov, Sov. J. Quan. Elec. 8 (2), 188 (1978).
[36] *Experimental data on shock compression and adiabatic expansion of condensed matter*, edited by R. F. Trunin (RFNC-VNIIEF, Sarov, 2001).
[37] M. Takeda, H. Ina, and S. Kobayashi, J. Opt. Soc. Am. 72, 156 (1982).
[38] L. M. Barker and K. W. Schuler, J. Appl. Phys. 45 (8), 3692 (1974).
[39] A. Dewaele, J. Eggert, P. Loubeyre, and R. LeToullec, Phys. Rev. B 67, 094112 (2003).
[40] C. Kittel and H. Kroemer, *Thermal Physics*, 2nd ed. (W. H. Freeman and Co., San Francisco, CA, 1980).
[41] A. A. Brish, M. S. Tarasov, and V. A. Tsukerman, Sov. Phys. JETP 11, 15 (1960).
[42] S. T. Weir, A. C. Mitchell, and W. J. Nellis, Phys. Rev. Lett. 76 (11), 1860 (1996).
[43] M. Bastea, A. C. Mitchell, and W. J. Nellis, Phys. Rev. Lett. 86 (14), 3108 (2001).
[44] H. K. Mao, P. M. Bell, J. W. Shaner, and D. J. Steinberg, J. Appl. Phys. 49 (6), 3276 (1978).
[45] A. Saul and W. Wagner, J. Phys. Chem. Ref. Data 18 (4), 1537 (1989).
[46] H. Shimizu, T. Nabetani, T. Nishiba, and S. Sasaki, Phys. Rev. B 53 (10), 6107 (1996).
[47] W. B. Hubbard, M. Podolak, and D. J. Stevenson, in *Neptune and Trition*, edited by D. P. Cruikshank (University of Arizona Press, Tucson, AZ, 1995), pp. 109.

Table 1.

Listed below are the initial and final state values (determined at the shock breakout from the Al) of our shocked pre-compressed water samples. Initial pressures, P_0, are measured by ruby fluorescence,[44] while initial water densities, ρ_0, are calculated from P_0.[45] The shock velocities of Al are measured by VISAR. Particle (shock) velocity u_p and U_s, of water is determined by the fringe shift in the short step of the Al, where attenuation is less, for transparent (reflecting) water. For opaque and reflecting shots, u_p of water is determined by impedance match with the Al step.[33,34,36] Italicized values are calculated from the SESAME database[34] table 7150.[33] The final pressures and densities are calculated through the Rankine-Hugoniot relations.[27] Optical properties are given in the first column. Temperature estimates from the SESAME database,[34] table 7150,[33] are given in the final column. Uncertainties are listed below each measured value in parentheses.

Sample	P_0 GPa	ρ_0 g/cm^3	U_S (Al) μm/ns	U_S (H_2O) μm/ns	u_p (H_2O) μm/ns	P_f (H_2O) GPa	ρ_f (H_2O) g/cm^3	T_{SESAME} K
4-ns laser-shock pulse, VISAR interferometry at 532 nm only								
001212-13 transparent	0.75 (0.07)	1.199 (0.005)	10.3 (0.3)	8.7 (0.2)	4.5 (0.2)	47 (5)	2.47 (0.02)	*2100 (200)*
001213-12 opaque	0.93 (0.13)	1.229 (0.018)	13.0 (0.4)	*12.3 (0.3)*	7.4 (0.3)	112 (10)	3.08 (0.10)	*5500 (600)*
001222-6 reflecting (532)	0.68 (0.07)	1.195 (0.008)	17.3 (0.4)	17.6 (0.4)	12 (0.4)	250 (20)	3.75 (0.20)	*19000 (1700)*
1-ns laser-shock pulse, VISAR interferometry at 532 and 1064 nm								
011218-07 reflecting (1064)	1.02 (0.02)	1.242 (0.002)	15.5 (0.7)	14.9 (0.4)	10.0 (0.8)	185 (20)	3.77 (0.35)	*10800 (1700)*
011220-06 reflecting (1064) opaque (532)	0.40 (0.005)	1.127 (0.001)	15.1 (0.4)	15.3 (0.3)	9.8 (0.4)	169 (10)	3.14 (0.25)	*12500 (1200)*

Figure 1. Schematic interior model of Icy Giant planets Uranus or Neptune showing the approximate chemical makeup.[1] Left-hand side yields model pressure and temperature for the H-He envelope, icy mantle layer and rocky core for Neptune. The right-hand side shows the corresponding radii for each layer. It is expected that it is in the icy mantle that the quadrupole-strong magnetic field is produced.

Figure 2. Schematic cross-section of diamond-cell configuration used for laser-driven shock experiments on pre-compressed samples. Wide openings (300 μm radius holes) in tungsten carbide (WC) supports allow ample shock laser entry (35° opening) and VISAR access (18.5° opening). Thin diamonds are pushed together to apply pressure on a small sample of water (~30 nL) held in a hole within a stainless steel gasket 100 μm thick. An Al stepped foil is glued on the thinnest diamond and used to measure Al U_s with VISAR. A few ruby spheres are placed in the sample chamber for pre-compression pressure measurements via ruby fluorescence.[44] There is a 1000 Å Al flash coating on the laser-shock side of the thinnest diamond, and an anti-reflection coating on the thicker diamond for the VISAR measurement.

Figure 3. VISAR streaked image at 532 nm for sample 001212-13. The time duration for the shock record shown is ~5 ns and the vertical axis is ~200 microns. Al step breakouts are outlined in blue for the high and low steps. The water is transparent and continues to be after another shock enters the sample (green dashed line). A final shock enters the sample finally making the water opaque (red dotted outline).

Figure 4. VISAR streaked image at 1064 nm for sample 011218-07. Al step breakouts are shown for the short (A) and tall (B) steps. The time duration for the shock record shown is ~5 ns and the vertical axis is ~400 microns. This sample was pre-compressed to the ice VI[46] structure of water before undergoing shock conditions. Note that the intensity of light reflected after the short aluminum step (A) is still rather high, although not visible for the tall step (B). This is likely due to the decreased shock strength after going through ~10 microns of additional Al. Measured pressure and calculated temperature at A is ~ 185 GPa and 10,800 K. Variations in the reflectivity intensity along the spatial dimension is likely due to scattering of light from the ice VI crystals that grew in the pre-compressed water. **Inset.** Percent reflectivity as a function of time. In red (blue), a normalized lineout of the intensity used as a proxy for reflectivity, for the short (tall) step. There is a decaying reflectivity off the short Al step corresponding to ~30% reflectivity compared to ~80% reflectivity for the Al step.

Figure 5. Pressure versus temperature (T_{SESAME}) phase diagram for water. Samples that remained transparent at 532 nm (green outlined squares), opaque at 532 nm (green filled square), reflecting at 532 nm (green hatched square) and reflecting at 1064 nm (red hatched square, shaded region along 1 GPa pre-compression Hugoniot) are plotted with their calculated temperatures. Green dashed line between transparent samples (green outlined squares) shows transparency for the same sample after successive shocks (see description in text and Figure 3). The regions are separated by a thin, black, dashed line with a slope of ~ -12K/GPa. The thick, black, dashed line represents Neptune's isentrope.[47] Single-shock (pre-compressed to 1 GPa) Hugoniot of water is plotted as the

black (red) curve.[33,34] For reference, single-shock experiments on water observed to be transparent (open triangles[24]); opaque (closed triangles[22]); and reflecting (shaded region above ~100 GPa along single-shock Hugoniot[21]). The P-T points accessed by recent shock-reverberation experiments[7] are shown in blue circles. Along the right-hand axis, we plot the electronic conductivity, σ_e, as thin, dotted, black lines representing the 1, 10, 100 and 1000 $(\Omega\text{-cm})^{-1}$ contours.

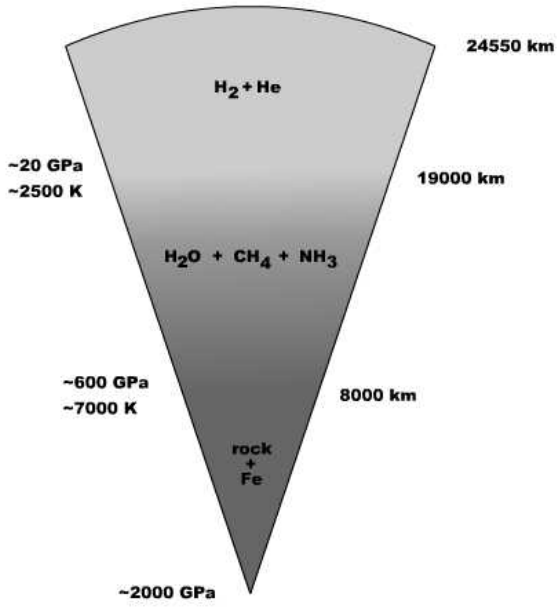
24550 km
H_2 + He
~20 GPa
~2500 K
19000 km
H_2O + CH_4 + NH_3
~600 GPa
~7000 K
8000 km
rock
+
Fe
~2000 GPa

Figure 1.

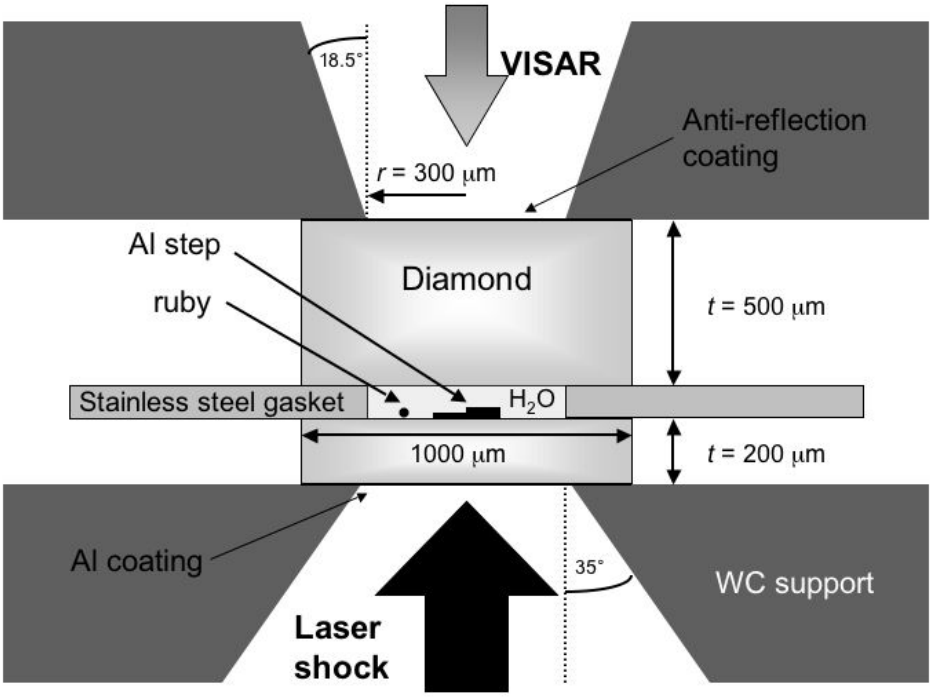
18.5°
VISAR
Anti-reflection coating
r = 300 μm
Al step
ruby
Diamond
t = 500 μm
Stainless steel gasket
H2O
1000 μm
t = 200 μm
Al coating
35°
WC support
Laser shock

Figure 2.

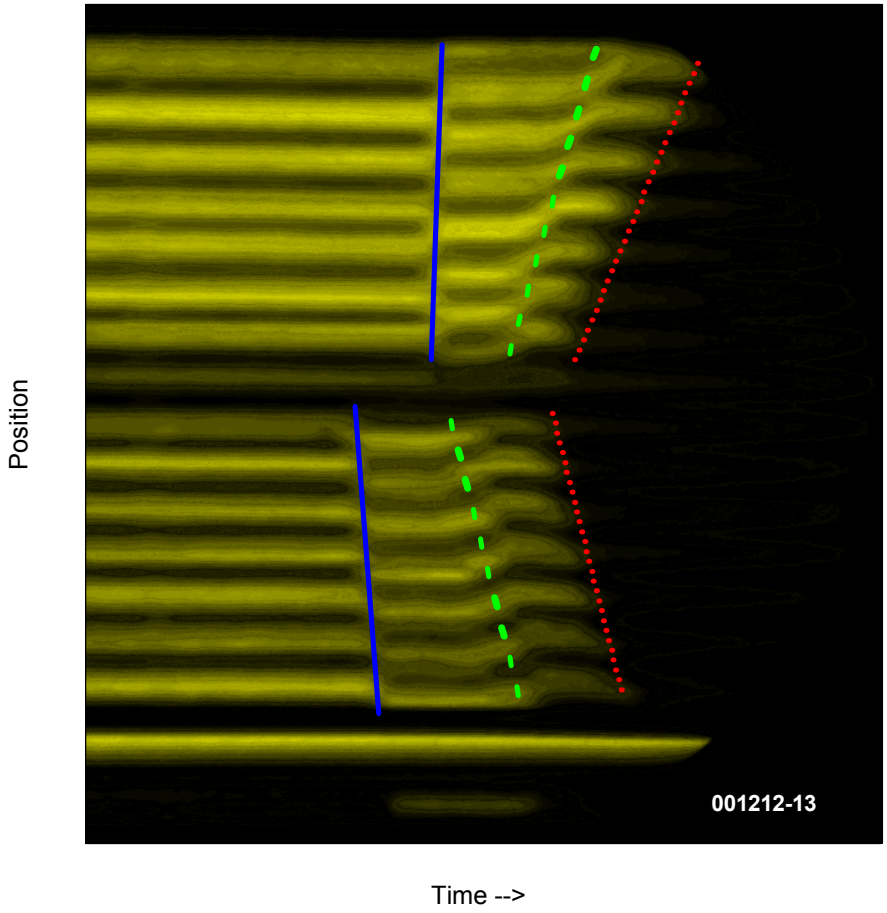

Figure 3.

?????????????????Where did the visar image go?????????????????

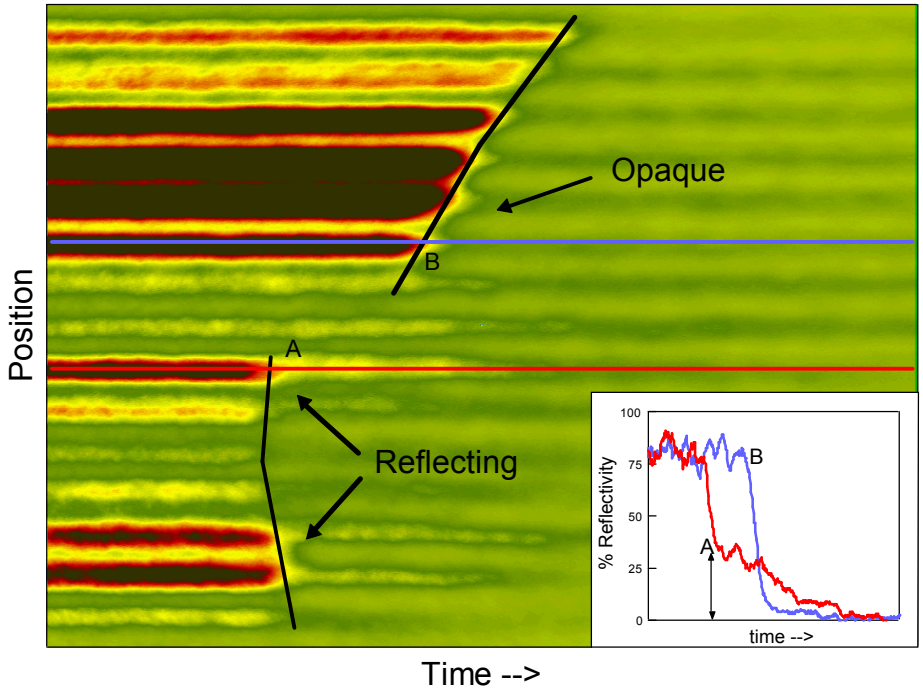

Figure 4
????????????????? Where did the visar image go ?????????????????

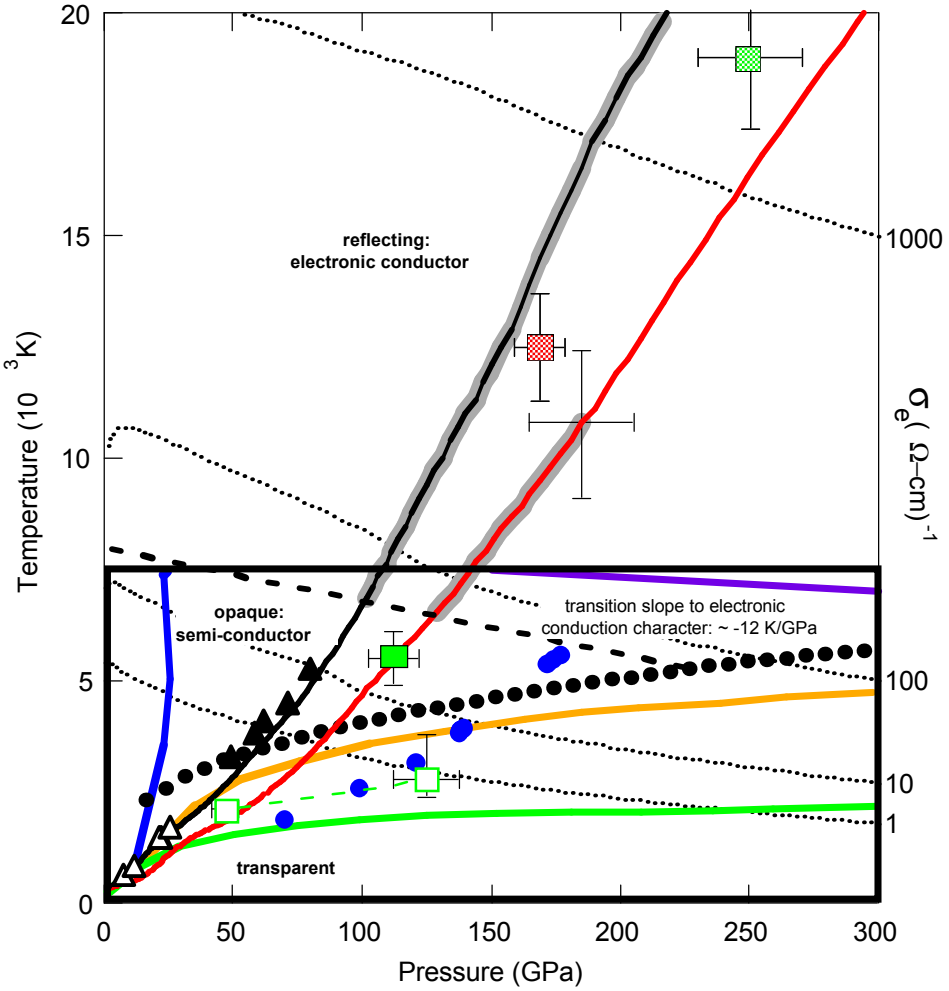

Figure 5

Remove heavy black box, rmove ionic, superionic boundaries, since we don't discuss them in the paper, Change the Neptune isentrope to a curve, not the black boxes. Increase font size on the labels in the figure